J Polym Environ (2012) 20:1052–1062
DOI 10.1007/s10924-012-0508-4

ORIGINAL PAPER

Dispersion and Reinforcing Potential of Carboxymethylated Nanofibrillated Cellulose Powders Modified with 1-Hexanol in Extruded Poly(Lactic Acid) (PLA) Composites

C. Eyholzer · P. Tingaut · T. Zimmermann · K. Oksman

Published online: 29 July 2012

Abstract Bionanocomposites of poly(lactic acid) (PLA) and chemically modified, nanofibrillated cellulose (NFC) powders were prepared by extrusion, followed by injection molding. The chemically modified NFC powders were prepared by carboxymethylation and mechanical disintegration of refined, bleached beech pulp (c-NFC), and subsequent esterification with 1-hexanol (c-NFC-hex). A solvent mix was then prepared by precipitating a suspension of c-NFC-hex and acetone-dissolved PLA in ice-cold isopropanol (c-NFC-hex$_{sm}$), extruded with PLA into pellets at different polymer/fiber ratios, and finally injection molded. Dynamic mechanical analysis and tensile tests were performed to study the reinforcing potential of dried and chemically modified NFC powders for PLA composite applications. The results showed a faint increase in modulus of elasticity of 10 % for composites with a loading of 7.5 % w/w of fibrils, irrespective of the type of chemically modified NFC powder. The increase in stiffness was accompanied by a slight decrease in tensile strength for all samples, as compared with neat PLA. The viscoelastic properties of the composites were essentially identical to neat PLA. The absence of a clear reinforcement of the polymer matrix was attributed to poor interactions with PLA and insufficient dispersion of the chemically modified NFC powders in the composite, as observed from scanning electron microscope images. Further explanation was found in the decrease of the thermal stability and crystallinity of the cellulose upon carboxymethylation.

Keywords Nanofibrillated cellulose · Polylactic acid · Esterification · Extrusion · Bio-nanocomposites

C. Eyholzer · P. Tingaut · T. Zimmermann (✉)
Applied Wood Materials Laboratory, Empa, Swiss Federal Laboratories for Materials Science and Technology, Dübendorf, Switzerland
e-mail: Tanja.Zimmermann@empa.ch

C. Eyholzer · K. Oksman
Division of Materials Science, Luleå University of Technology, Luleå, Sweden

Introduction

Polylactic acid (PLA) is an aliphatic polyester with high strength and stiffness that can be made from annually renewable resources, like starch from corn or potato, and sugar from cane or beet. Being a thermoplastic, it is easily processed on standard plastic equipment to yield molded parts, films or fibers. Due to its biocompatibility and biodegradability, PLA is suitable for medical devices or for use in the industrial packaging field [1, 2].

The isolation and use of cellulose nanostructures and their application in composite materials has gained increasing attention due to their inherent properties like high strength and stiffness combined with low weight, biodegradability and renewability [3]. Their beneficial mechanical properties arise from β-1,4 linked glucopyranose chains, aligned into highly ordered (crystalline) domains by intra- and intermolecular hydrogen bonds. These crystallites are linked by amorphous domains to form bundles of fibrils [4]. Over the last years, two categories of nanocelluloses have been mainly used in order to reinforce a PLA matrix: cellulose nanowhiskers (CNW) and nanofibrillated cellulose (NFC). CNW are mostly obtained by acid hydrolysis of cellulose pulp from wood, or other sources of cellulose, such as algae, bacteria, tunicates or wheat. The chemical treatment dissolves the amorphous fraction of cellulose and needle shaped crystallites are isolated [5–7]. Mechanical isolation of pulp (usually applied in combination with a chemical, mechanical

or enzymatic pretreatment) results in breakup of the cellulose fibers and yields semi-crystalline fibrils and fibril bundles with diameters in the range between 3.5 and 100 nm, called NFC [8]. Due to their beneficial mechanical properties and their inherent biodegradability and biocompatibility, CNW and NFC are qualified for the development of nanocomposites with PLA. However, due to their large, hydrophilic surface area [4, 8], these nanomaterials tend to undergo agglomeration when compounding with hydrophobic polymers. In response, several strategies have been examined to overcome this issue in composites with PLA and the resulted mechanical properties are listed in Table 1.

In first experiments, slurries containing CNW in N,N-dimethyl acetamide/lithium-chloride (DMAc/LiCl) and a maleic anhydride coupling agent were directly fed into a PLA melt during extrusion. The results indicated that the CNW had a positive effect on all mechanical properties (stiffness, strength and strain) of the composites, even though the additives showed tendency for agglomeration [9]. In a subsequent study, aqueous suspensions of CNW or NFC in combination with polyethylene glycol (PEG) were fed into the PLA melt. Again, the formation of agglomerates could not be avoided [10]. Nanocomposites were also prepared by solution casting. CNW were freeze-dried from an aqueous suspension, after solvent exchange to *tert*-butanol and after modification with a surfactant. The powders were then redispersed in chloroform and the suspensions were mixed with dissolved PLA, followed by evaporation of the solvent. The surfactant considerably improved dispersion of the CNW in the PLA matrix compared to the unmodified CNW, as was observed by transmission electron microscopy (TEM). However, agglomeration of CNW was not completely prevented. In addition, the surfactant clearly decreased the storage modulus of the PLA matrix [11]. Similar results were obtained when surfactant modified, freeze-dried CNW were extruded with PLA. Even though, the surfactant greatly improved the dispersion of CNW in the PLA matrix (compared to unmodified CNW), the composites did suffer from a slight decrease in stiffness and strength, caused by the plasticizing effect of the surfactant [12, 13]. Extrusion of PLA with a masterbatch of CNW and polyvinyl alcohol (PVOH) (directly fed to the melt as solution or as a solid mixture after freeze-drying) resulted in phase separation of the immiscible polymers. The CNW were located predominantly in the discontinuous PVOH phase and therefore only a limited increase in tensile modulus and strength of PLA was observed [12]. Later, nanocomposites were prepared by gradually adding PLA to a thoroughly dispersed suspension of unmodified NFC in acetone, followed by solution casting. The films were then melt-kneaded in a rotary roller mixer and hot-pressed. This procedure seems somewhat irritating, as unmodified NFC is expected to show instantaneous sedimentation in the described 9:1 w/w acetone/water mixture. Nevertheless, microscopic images showed a homogeneous distribution of NFC in the fully amorphous PLA matrix and tensile tests showed an increase of 25 and 16 % for modulus and tensile strength, respectively [14]. A very similar procedure was then applied to reinforce a semi-crystalline PLA with unmodified NFC. The thin film composites were either quenched in liquid nitrogen or annealed in a hot press at 100 °C to obtain fully amorphous or crystallized composites, respectively. The tensile moduli and strengths of the amorphous composites were approximately in the same range as those of the precedent experiment, while the crystallized samples showed slightly higher values. Dynamic mechanical analysis (DMA) showed a clear increase in storage modulus above the glass transition for composites containing unmodified NFC compared to neat PLA, especially for

Table 1 Overview on modulus, tensile strength and elongation to break of selected composites containing NFC or whiskers in PLA

Source	Filler	Additives	Modulus (GPa)		Strength (MPa)		Elongation to break (%)	
			Neat PLA	Composite	Neat PLA	Composite	Neat PLA	Composite
Oksman et al. [9]	Whiskers	DMAc/LiCl PLA-MA	2.9 ± 0.1[a]	3.9 ± 0.3	40.9 ± 3.2[a]	77.9 ± 6.7	1.9 ± 0.2[a]	2.7 ± 0.5
Mathew et al. [10]	NFC	PEG	2.0 ± 0.2	2.3	58 ± 6	59 ± 2	4.2 ± 0.6	3.3 ± 0.2
	Whiskers	PEG		2.1		47 ± 5		5.4 ± 1.8
Bondeson et al. [12]	Whiskers	Beycostat surfactant	2.7 ± 0.1	3.1 ± 0.2	62.8 ± 1.0	52.4 ± 0.4	19.5 ± 9.7	3.1 ± 0.2
Bondeson et al. [13]	Whiskers	PVOH	3.3 ± 0.1	3.6 ± 0.3	71.9 ± 2.0	67.7 ± 0.8	3.4 ± 0.2	2.4 ± 0.2
Iwatake et al. [14]	NFC	–	3.4	4.3	56.2	66.0	N.a.	N.a.
Suryanegara et al. [15]	NFC	–	3.3 ± 0.2[b]	3.9 ± 0.1[b]	57.7 ± 1.5[b]	63.4 ± 1.1[b]	6.8 ± 2.1[b]	2.5 ± 0.2[b]
		–	4.0 ± 0.1	4.6 ± 0.1	60.9 ± 1.6	64.4 ± 0.8	3.1 ± 0.4	2.0 ± 0.1
Jonoobi et al. [17]	NFC	–	2.9 ± 0.6	3.6 ± 0.7	58.9 ± 0.5	71.2 ± 0.6	3.4 ± 0.4	2.7 ± 0.1
c-NFC-hex sm 5 % w/w		–	3.6 ± 0.1	3.7 ± 0.1	66.2 ± 1.6	59.6 ± 0.8	4.1 ± 1.3	3.3 ± 0.6

The loading of nanoparticles in each composite was 5 % w/w

[a] Values for PLA extruded with indicated additives

[b] Values for purely amorphous PLA

crystallized samples [15]. An increase in storage modulus above the glass transition was also found for composites obtained by solution casting of a mixture of acetylated NFC and PLA from chloroform. Interestingly, for the same fibril loadings, the acetylated NFC showed a lower reinforcement in the rubbery plateau than unmodified NFC, which was attributed to a reduced number of hydrogen bonds that could be formed due to the acetyl groups [16]. In a most recent study, unmodified NFC was solvent exchanged from water to acetone before mixing with dissolved PLA. Again, the mixture was evaporated and dried before extrusion. An increase in modulus of 25 % and strength of 20 % was observed. However, scanning electron images still proved the formation of agglomerates within the composites [17].

Over all as shown in Table 1, the reinforcement of PLA with CNW and NFC led to a maximum increase in stiffness of 42 and 25 %, respectively. Most of the studies did not show any improvement in strength, which was mainly attributed to the poor filler dispersion and interaction between the nanofibers and the PLA. Interestingly, the highest increase in strength and strain reported so far has been measured for unmodified CNW and NFC [9, 17].

It is therefore not surprising that in all composites containing PLA presented so far, at least to a certain extent, NFC agglomeration was observed. However, as generally emphasized, perfect dispersion in the matrix to yield a large interfacial area and strong interaction between the components is crucial for exploiting the full reinforcing potential. In addition, the proposed preparation procedures have involved either a liquid feeding of the components to the extruder or a solution casting step.

Therefore, a simple procedure for the development of nanocomposites containing perfectly dispersed NFC or CNW (provided in dry form) in PLA, allowing the scale up to industrially competitive processes, has not been presented so far. We showed in an earlier study [18] that carboxymethylated NFC (c-NFC) powder can be redispersed in water after drying and therefore, it is interesting to see if this cellulose type can be even redispersed in a non-polar polymer during the extrusion process. Accordingly in this study, c-NFC in dry powder form was used as starting material and its carboxymethyl groups were esterified with 1-hexanol in order to increase the compatibility at the fiber-polymer matrix interface. Nanocomposites were prepared by compounding extrusion and the test samples were injection molded. The fractured surfaces of the tensile tested samples were analyzed by scanning electron microscopy (SEM) to study the dispersion of the NFC in PLA. The mechanical properties of the nanocomposites were analyzed by tensile tests, dynamic mechanical analysis (DMA) and melt shear tests and compared to neat PLA samples.

Materials and Methods

Materials

Refined, bleached beech pulp (RBP) was provided by J. Rettenmaier & Söhne GmbH (Rosenberg, Germany) as an aqueous suspension (Arbocel B1011). The dry material content of the suspension was measured by gravimetry to 12.4 % w/w. The Kappa number and the hemicellulose content were 1.0 and 7.07 %, respectively, as determined by chemical analysis. Mono-chloroacetic acid (sodium salt, purity $\geq$98 %, M = 116.48 g/mol), 1-hexanol (purity $\geq$98 %, M = 102.17 g/mol) and sulfuric acid (H_2SO_4, p.a. 95–97 %, M = 98.08 g/mol) were purchased from Merck. Sodium hydroxide (NaOH, purity $\geq$98 %, M = 40.0 g/mol) and dichloromethane (CH_2Cl_2, purity $\geq$98 %, M = 84.93 g/mol) were purchased from Fluka and Carl Roth GmbH. Polylactic acid (PLA, 2002 D grade, Nature Works^{TM}) was provided by Cargill Dow LCC (Minnetonka, MN, USA).

Sample Preparation

Synthesis of Carboxymethylated NFC (c-NFC)

Carboxymethylation of RBP was performed following an earlier protocol [18] with slight modifications: 806 g of RBP (corresponding to 100 g of dry cellulose) was dispersed in 4.5 L of a 3:5 v/v ethanol/isopropanol mixture in a 10 L glass reactor. After a swelling time of 4 days, the RBP was activated by dropping 493 g of a 5 % w/w aqueous NaOH into the mixture. 53.9 g of mono-chloroacetic acid were added. The temperature was set to 60 °C and the reaction conducted for 2 h. (Fig. 1). The resulting suspension was washed with a 1/1 v/v mixture of a 0.05 M aqueous acetic acid solution and a 5/3 v/v isopropanol/ethanol mixture, and finally dispersed in 9.5 L of a 0.01 M NaOH. Mechanical disintegration was done using a high-shear homogenizer (Microfluidizer type M-110Y, Microfluidics Corporation, USA). Two chamber setups were used. The suspensions were pumped 3 times through $H230Z_{400\mu m}$ and $H30Z_{200\mu m}$ chambers, followed by another 3 passes through $H30Z_{200\mu m}$ and $F20Y_{75\mu m}$ chambers. The c-NFC suspension was then solvent-exchanged to isopropanol (centrifugation at 5,000 rpm for 15 min, followed by discarding the supernatant and dispersion of the c-NFC sediment in isopropanol; procedure was repeated three times). The c-NFC was finally dried from isopropanol at 60 °C under stirring to avoid hornification (irreversible agglomeration) [18]. A degree of substitution (DS) of 0.23 was determined by conductometric titration (average of three measurements).

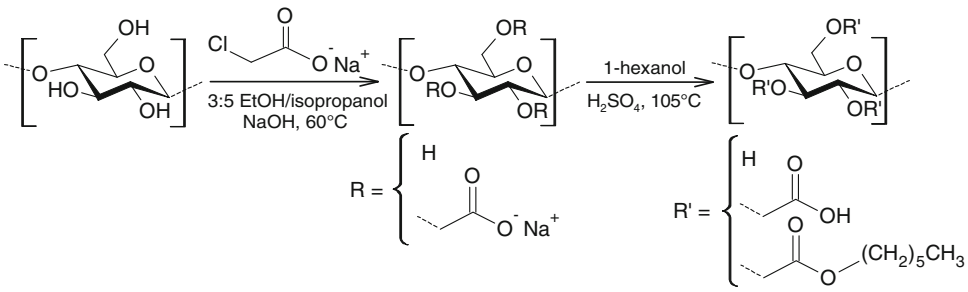

Fig. 1 Synthesis of c-NFC (*center*) and c-NFC hexanoate (*right*). The DS of functional groups R and R' were determined by conductometric titration: $DS_{COOH} = 0.09$ and $DS_{hex} = 0.14$

Synthesis of c-NFC Hexanoate (c-NFC-hex)

40 g of dried c-NFC was dispersed in 1.0 L of 1-hexanol using a high-shear mixer (T 25 basic, IKA-Werke, Stauffen, Germany) in a 2 L glass reactor, equipped with a mechanical stirrer and reflux cooler. 2 mL of H_2SO_4 was added with a pipette. The reaction was conducted at 105 °C for 72 h (Fig. 1). The suspension was centrifuged at 5,000 rpm for 30 min. The sediment was washed twice with 700 mL of a 1/1 v/v acetone/0.001 M NaOH mixture and 3 times with pure acetone. Then, the c-NFC-hex was dried at 60 °C in an oven under frequent manual stirring.

The DS of the unreacted carboxymethyl groups was determined, using Eq. 1:

$$DS_{COOH} = \frac{n_{COOH}}{n_{AGU}} = n_{COOH}\left(\frac{m_0 + (n_{COOH} \cdot M_{hex})}{M_{AGU} + (DS_{c-NFC} \cdot M_{hex}) + (DS_{c-NFC} \cdot M_{cm})}\right)^{-1} \quad (1)$$

with n_{COOH} and n_{AGU} being the amount of free COOH groups (measured by conductometric titration), and the amount of anhydroglucose units, respectively. m_0 is the mass of the weighted sample of dry c-NFC hexanoate. M_{hex}, M_{AGU} and M_{cm} denote the molecular masses of the hexanoate group ($(CH_2)_5CH_3$, 85 g/mol), the anhydroglucose unit (162.14 g/mol) and the carboxymethyl group (57 g/mol). $DS_{c\text{-}NFC}$ denotes the DS of the c-NFC intermediate product (0.23). The final DS of free carboxymethyl groups and hexanoate groups were calculated using Eq. 2 to $DS_{COOH} = 0.09$ and $DS_{hex} = 0.14$, respectively:

$$DS_{hex} = DS_{c-NFC} - DS_{COOH} \quad (2)$$

Preparation of Solvent Mix PLA (c-NFC-hex$_{sm}$)

16.0 g of c-NFC-hex was dispersed in 400 ml of CH_2Cl_2 using a high-shear mixer. In a separate flask, 16.0 g of PLA was dissolved in 400 mL of acetone overnight. The mixtures were combined in a 1 L flask and homogenized using a high-shear mixer. CH_2Cl_2 was distilled off the suspension using a Rotavap and the remaining suspension was dropped into 2 L of ice-cold isopropanol. The precipitate was dried in an oven at 60 °C.

Compounding Extrusion

All materials were dried prior to extrusion at 50 °C overnight. A MEGALab 18 co-rotating twin-screw extruder (Coperion W&P, Stuttgart, Germany) containing 7 heating zones (set to 165; 170; 170; 180; 180; 190 and 200 °C, respectively) was used. The screw speed was set to 150 rpm.

In the first step, 3 different material combinations were prepared to make extruded masterbatches: 10/90 w/w c-NFC/PLA; 10/90 w/w c-NFC-hex/PLA and 10/90 w/w c-NFC-hex$_{sm}$/PLA. Neat PLA was subjected to the same process to ensure similar processing history. All extrudates were pelletized.

In the second step, the extruded masterbatch pellets were diluted with fresh PLA in order to obtain mixtures containing a total of 2.5, 5.0 and 7.5 % w/w of dry material (c-NFC/c-NFC-hex and c-NFC-hex$_{sm}$, respectively). The mixtures were extruded using the same parameters and subsequently pelletized.

Injection Molding

The prepared composites and the PLA were injection molded using a Haake MiniJet laboratory injection molding machine (Thermo Scientific, Karlsruhe, Germany). Dog-bone specimens according to ASTM D638-2003 standard, type 5 (thickness 3.3 mm, width 3.2 mm, length 60 mm, parallel length l_0 20 mm) and flat discs (diameter 32 mm, thickness 1.6 mm) were injection molded. The following parameters for dog-bone specimens and flat discs (in brackets) were used: cylinder temperature 200 °C (200 °C), mold temperature 60 °C (80 °C), injection pressure 500 bar (600 bar), injection time 30 s (30 s), hold pressure 100 bar (100 bar), hold time 60 s (60 s).

Measurements

Tensile Tests

Modulus of elasticity (MOE) and nominal tensile strength were determined according to EN ISO 527-1:1996 with slight modifications. A Universal Testing System (Zwick 1474, Ulm, Germany), equipped with a 20 kN load cell was used. The samples were conditioned for 1 week at 35 % relative humidity and 20 °C. Elongation of the samples was measured by mechanical strain detection. MOE values were determined by the slope of the linear interpolation line of the curves between 0.1 and 0.3 % strain. The initial cross head speed was set to 1 mm/min and increased to 2 mm/min after the determination of the MOE to reduce creeping of the samples. For each sample, 10 replicates were measured.

Dynamic Mechanical Analysis (DMA)

Viscoelastic properties of injection molded samples were studied by using a RS IIIa Rheometrics System Analyzer (TA Instruments, Delaware, USA) in three point bending mode. The composite flat discs were cut into rectangular specimens with 10.0 mm width and 40.0 mm length and were conditioned for 1 week at 20 °C and 35 % relative humidity.

Dynamic heating scans were performed from 30 to 140 °C at a heating rate of 2 °C/min with an initial static force of 75 g. The heating scans were followed by 2 min of isothermal equilibration at 140 °C and dynamic cooling scans at a cooling rate of 2 °C/min with an initial static force of 2 g. The static force in all scans was set 15 % higher than the dynamic force. Initial load strain and upper limit for the applied load strain were set to 0.05 and 0.1 %, respectively. All measurements were done at a frequency of 1 Hz. Purge gas was dry air over the whole temperature range.

Melt Flow Index (MFI)

Melt flow indexes (MFI) of neat PLA and composites were measured using a MI-1 apparatus (Goettfert, Buchen, Germany). The specimens were melted at 190 °C for 2 min. The mass of the piston was 2.16 kg. The mass of the polymer composites that flowed through the capillary was measured after 30 s. An average of 5 measurements was calculated for each sample.

Shear Tests

The viscoelastic properties of the injection molded flat disc samples in shear (storage modulus G', loss modulus G" and viscosity γ) were measured using an ARES, Rheometric Scientific Inc. (New Jersey, USA) in parallel plate geometry (diameter 50 mm). Dynamic frequency sweep tests were performed at 180 and at 200 °C. The flat discs were melted and compressed until fully occupying the area of the plates (disc gap between 0.8 and 1.2 mm). A delay of 180 s after the preload ensured complete relaxation of the samples before the tests. A shear strain of 1.0 % with frequencies from 0.08 to 80 Hz (0.50265–502.65 rad/s) was applied and 9 points per decade were recorded. Two specimens per sample were measured and the values were averaged.

Scanning Electron Microscopy (SEM)

Fractured dog-bone tensile specimens were cut with a razor blade to obtain cubes of 3 mm edge length. The cubes were mounted on a sample holder. The fractured surfaces were sputter coated with a platinum layer of 7.0 nm (BAL-TEC MED 020 Modular High Vacuum Coating System with integrated quartz crystal film thickness and coating rate measuring, BAL-TEC AG, Liechtenstein) in Ar as a carrier gas at $5 \times 9 \times 10^{-2}$ mbar. Images were recorded in a FEI NovaNanoSEM (FEI Company, Hillsboro, OR, USA), equipped with a Schottky field emission gun. The following parameters were used: acceleration voltage of 5.0 kV and working distance of 5.0 mm. Of each sample, two specimens were examined.

Results and Discussion

Materials Preparation

Figure 1 presents the synthesis of c-NFC hexanoate. We started with a carboxymethyl cellulose (c-NFC) powder with a DS a 0.23. The esterification reaction of c-NFC was performed after redispersion of the powder in 1-hexanol. After reaction and proper washing procedures, a DS of 0.14 was determined for c-NFC-hex, therefore confirming that more than 60 % of the original carboxyl acid functions were esterified.

After the reaction, when left without stirring, the c-NFC-hex in the mixture sedimented within a couple of minutes. During washing of c-NFC-hex with 1/1 v/v acetone/0.001 M NaOH, foam generation was observed, which could be the result of the formation of micellar structures of the alkyl side chains in aqueous medium. In pure acetone, c-NFC-hex did not form a stable suspension but sedimented after some minutes. The tendency towards sedimentation suggests the presence of agglomerates of nanofibrillated cellulose and must be kept in mind when discussing the results of the following measurements.

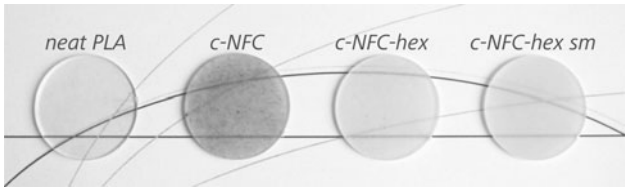

Fig. 2 Photographs of flat discs (thickness 1.6 mm) of neat PLA and composite samples containing 5.0 % w/w of fibrils. Dark coloration was attributed to thermal degradation of the matrix and fibrils

The various products (c-NFC, c-NFC-hex powder and c-NFC-hex$_{sm}$) were extruded to yield three different composites, each with 3 loadings of fibrils, i.e. 2.5, 5.0 and 7.5 % w/w of fibrils. The extrudates were cut to pellets and injection molded to yield dog-bone shaped tensile testing samples and flat disc samples for DMA and melt shear measurements. While neat PLA samples were almost colorless and transparent, the composite samples showed the formation of a yellowish color (Fig. 2). This coloration was faint for composites containing c-NFC-hex$_{sm}$ and c-NFC-hex but clearly more pronounced for composites containing c-NFC (almost dark brown color). In addition, the transparency of the samples was also reduced in the same order and in some samples agglomerates, big enough to be detected by naked eye, were observed.

Characterization of Materials

Figure 3 (left) shows the modulus of elasticity (MOE) of neat PLA (white column) and the composites containing c-NFC, c-NFC-hex and c-NFC-hex$_{sm}$ (light, medium and dark gray columns, respectively), obtained from tensile tests. As it can be seen, only small differences between the MOE values of the different samples were measured. At the highest loading of 7.5 % w/w, MOE values increased only 10 % compared to neat PLA showing a modulus of 3.61 GPa, while for lower loadings the effect was even less pronounced. No differences in modulus were observed for composites containing different types of fibrils. Similar behavior was observed when analyzing the tensile strength of the samples (Fig. 3, right). Neat PLA showed a tensile strength of about 66 MPa and again, the values of the composites showed little differences. The data suggests that with increasing loading of the fibrils the tensile strength even decreased, which was most pronounced for the composite containing c-NFC. From these results we must deduce that the reinforcing potential of the fibrils was not exploited and the fibrils acted as filler rather than as a reinforcing agent.

Nevertheless, moduli and tensile strengths measured for the developed composites are in the same range as the mechanical properties for composites containing 5 % w/w of NFC or CNW in earlier reports (Table 1). It must however be considered that the values reported in this table have to be taken with care, as they are affected by the chosen test parameters (test method, sample dimensions, load cell, cross-head speed, etc.).

The results from tensile tests were further confirmed by DMA experiments. Figure 4a shows heating scans of the neat PLA (green dots) and the composites containing 7.5 % w/w of c-NFC, c-NFC-hex and c-NFC-hex$_{sm}$ (purple, olive and yellow dots, respectively). Neat PLA is in a glassy state at room temperature, with a storage modulus (top) of approximately 3 GPa. Upon heating, the tan δ curve (bottom) peaked at approximately 60 °C, indicating the transition from a glassy to a rubbery state. The transition was followed by a short rubbery plateau of storage modulus up to 85 °C. Above this temperature, a faint drop in storage modulus was observed for neat PLA. This drop was attributed to the relaxation of molded-in stresses from

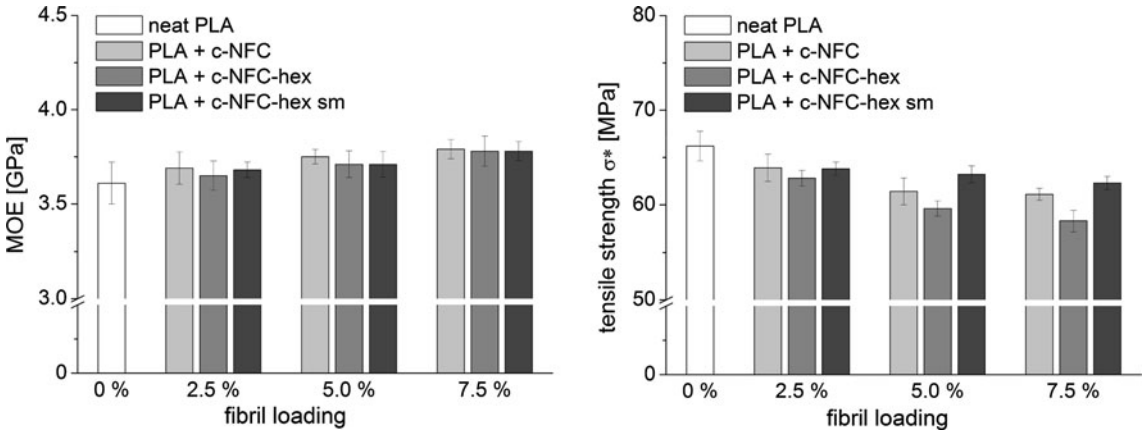

Fig. 3 Modulus of elasticity (MOE) (*left*) and tensile strength (*right*) for neat PLA and composites containing c-NFC, c-NFC-hex or c-NFC-hex$_{sm}$ in dependence of fibril loadings in w/w %, obtained from tensile testing experiments. A linear scale was chosen to visualize the small differences in MOE between samples

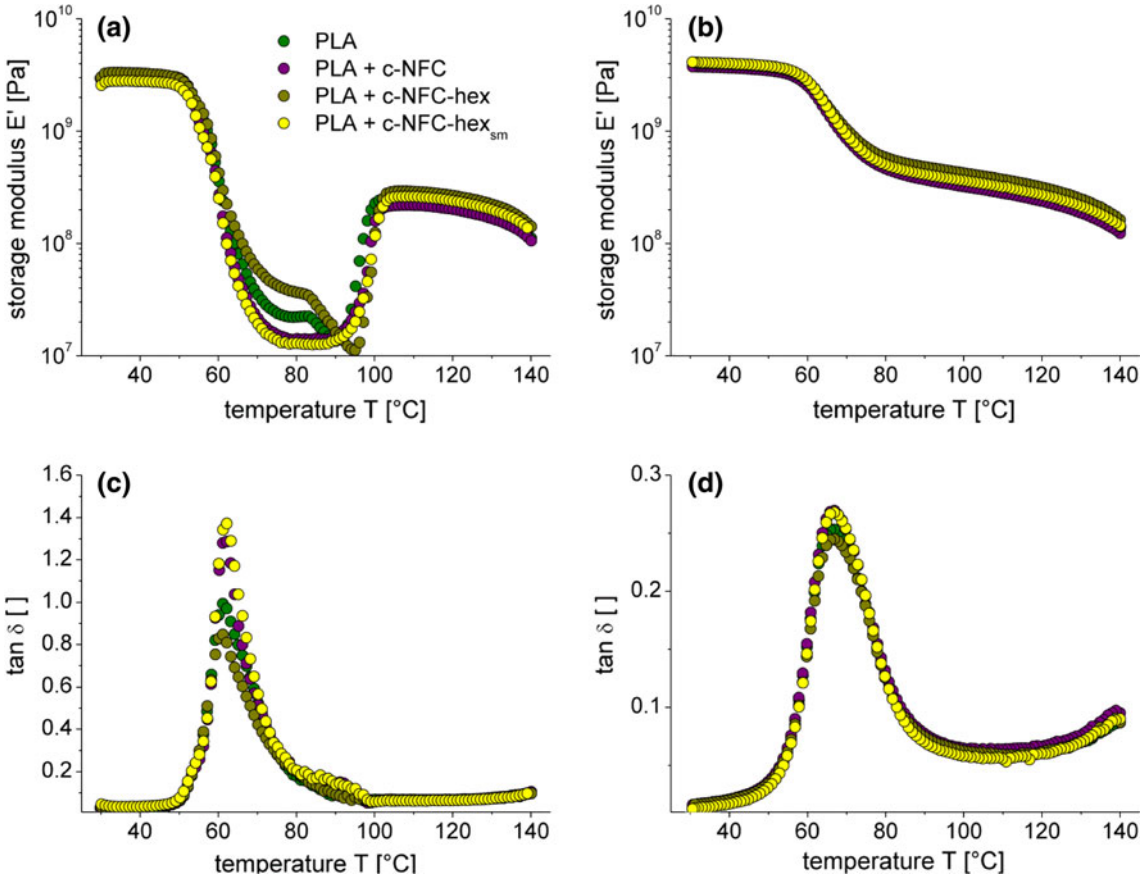

Fig. 4 Dynamic mechanical analysis (DMA) test heating scan (*left*) and cooling scan (*right*) of neat PLA and composites containing 7.5 % w/w of c-NFC, c-NFC-hex or c-NFC-hex$_{sm}$ in three-point bending geometry. The *curves* show the storage modulus E' (**a, b**) and tan δ (**c, d**) in dependence of temperature, recorded at a frequency ω of 1 Hz. For better visualization, the tan δ scale in (**d**) was enlarged

injection molding. Above 90 °C, the storage modulus showed an increase of more than one decade, indicative for a crystallization process of the semicrystalline polymer matrix. At 100 °C, a second, broad, plateau was reached, which slowly declined at higher temperatures approaching the melting temperature. The peak position and form was similar for all tested materials, only the peak height changed, which is indicative for the amount of molecules participating in the relaxation. Nevertheless, the fact that the peak position did not change can be interpreted as lack of interaction between the NFC and PLA.

The storage moduli of the composites showed basically the same temperature dependence as neat PLA. Minor differences were observed in the relaxation of the molded-in stresses, indicating slightly different cooling profiles (as samples were ejected manually from the mold, this could not be avoided completely).

Figure 4b shows the subsequent cooling scan of neat PLA (green dots) and composites with 7.5 % w/w NFC (purple, olive and yellow dots, respectively). A continuous rubbery plateau was found for all curves with a slight increase in storage moduli towards lower temperatures. Upon further cooling, the samples changed into a glassy state, indicated by the tan δ peak around 60 °C. Clearly, all the samples showed almost the same values in both scans, suggesting very similar viscoelastic properties in the examined temperature range. As already observed for the tensile tests, the results obtained with DMA confirmed that the fibrils did not lead to a significant increase in stiffness of the composites, and no evidence was seen on restriction of molecular movement of the PLA which is also indicative for poor interaction between the PLA and the nanofibers, chemically modified or not.

In addition to the measurements done at the glassy and rubbery states of PLA, the composites were also analyzed in their melted form with the aim to indirectly get information about the dispersion quality of the nanofibers inside the polymeric matrix, as the melt flow is expected to decrease with the addition of nanofibers and their dispersion. Figure 5 shows the melt flow index (MFI) of neat PLA and the composites in dependence of the type and loading of fibrils. For neat PLA (white column), an MFI of

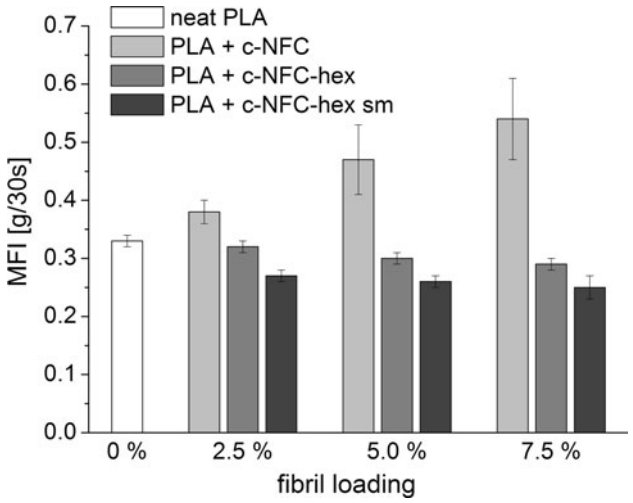

Fig. 5 Melt flow index (MFI) for neat PLA and composites containing c-NFC, c-NFC-hex or c-NFC-hex sm in dependence of fibril loadings in % w/w

0.33 was measured. For composites containing c-NFC (light gray columns), the MFI increased with the fibril loading. This is an indication for degradation of the PLA matrix, leading to a reduction of the PLA chain length [19] and therefore to a lower viscosity. In contrast, the MFI of composites containing c-NFC-hex (medium gray columns) and c-NFC-hex$_{sm}$ (dark gray columns) showed a faint decrease with higher fibril loadings, which indicates that a better fiber dispersion was obtained for these nanofibers, especially for the solvent mixed composites.

These results were confirmed by shear tests in parallel plate geometry. Figure 6 shows frequency scans of neat PLA and composite samples containing 7.5 % of fibrils at 180 °C (left) and 200 °C (right), displaying the shear storage modulus G' (top), shear loss modulus G" (center) and the viscosity γ (bottom) in dependence of the angular frequency ω. At 180 °C, G' and G" of the neat PLA melt (green dots) increased over several decades with increasing

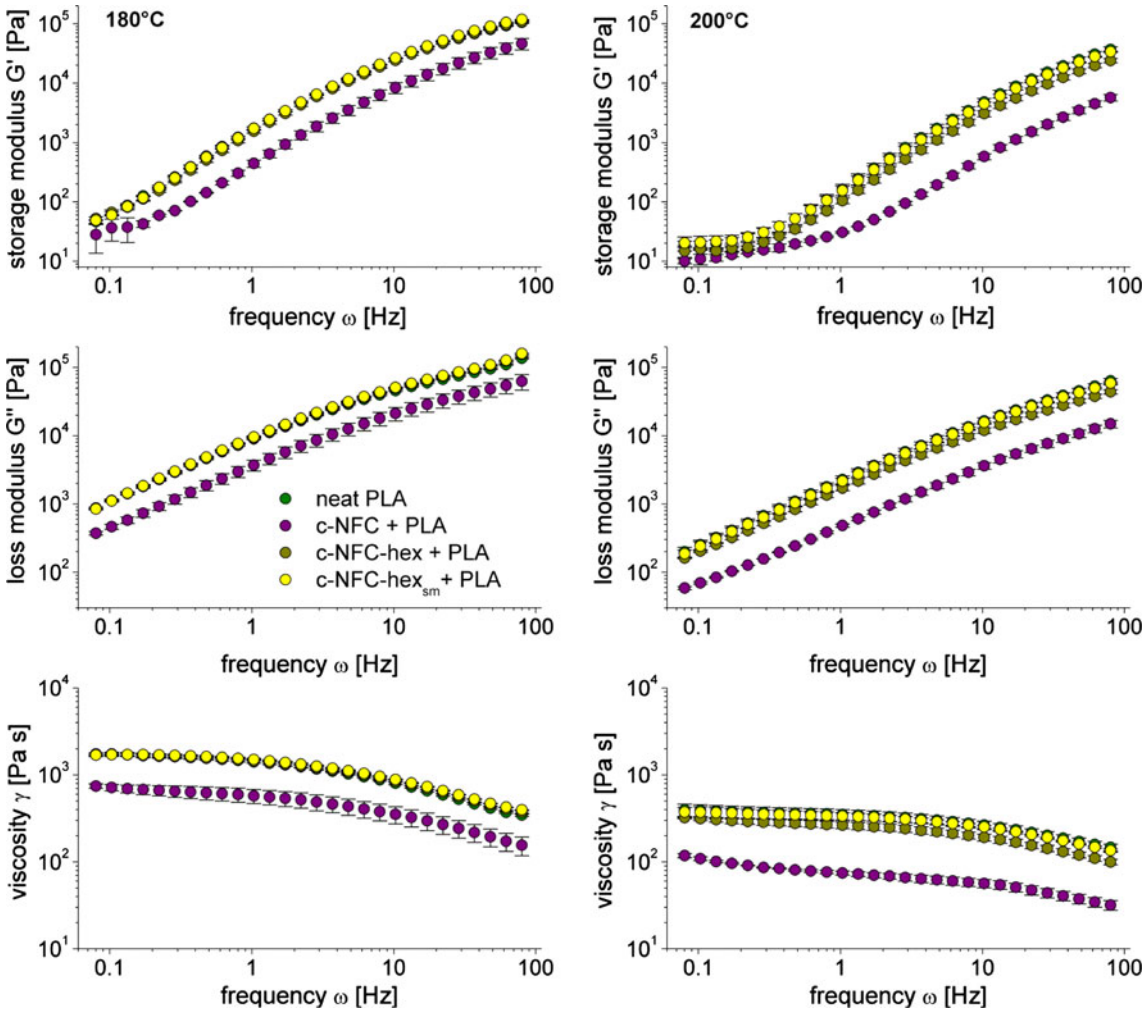

Fig. 6 Dynamic mechanical analysis (DMA) melt shear test in parallel plate geometry of neat PLA and composites containing 7.5 % w/w of c-NFC, c-NFC-hex or c-NFC-hex$_{sm}$. The figures show the storage modulus G' (*top*), loss modulus G" (*center*) and viscosity γ (*bottom*) in dependence of the frequency ω of the samples at 180 °C (*left*) and 200 °C (*right*)

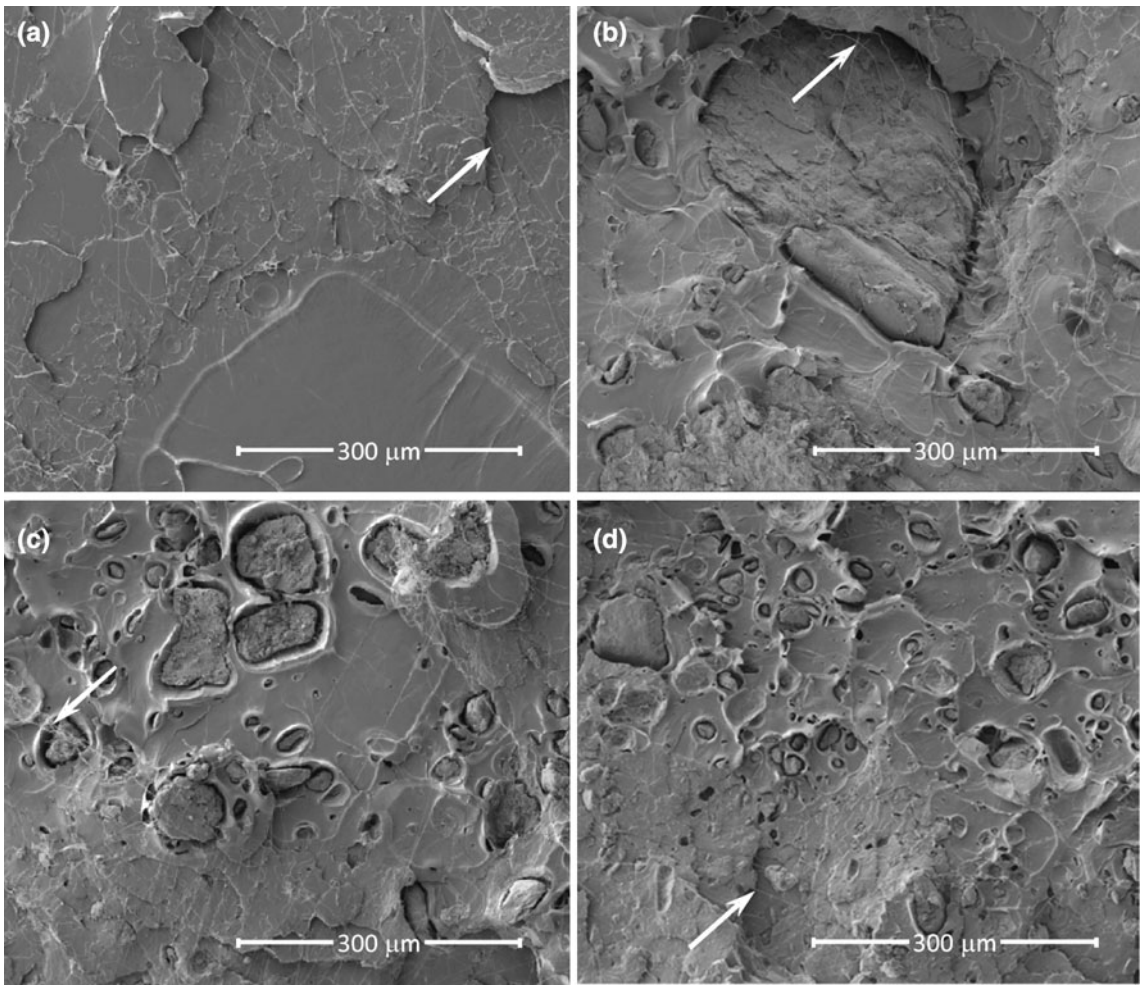

Fig. 7 Scanning electron microscopy (SEM) images of **a** neat PLA and composites containing PLA and 7.5 % w/w of **b** c-NFC, **c** c-NFC-hex and **d** c-NFC-hex sm. The images show fracture surfaces of tensile testing specimens. Arrows indicate polymer fibrils. Magnifications are approximately 130×

the frequency from 0.08 to 80 Hz. The gel point (G' = G") was not reached in the whole frequency range measured. The viscosity of the neat PLA melt was almost constant at 2 kPa s for low frequencies and decreased with higher frequencies (shear thinning effect). Almost identical responses for G', G" and γ were obtained for composites containing c-NFC-hex (olive dots) and c-NFC-hex$_{sm}$ (yellow dots). Composites containing c-NFC (purple dots) showed the same behavior with clearly lower values. The same trends were observed at 200 °C, with lower values for all samples measured.

The fractured surfaces of tensile test specimens of neat PLA (Fig. 7a) and composites containing 7.5 % w/w of c-NFC (Fig. 7b), c-NFC-hex (Fig. 7c) and c-NFC-hex$_{sm}$ (Fig. 7d) were analyzed using scanning electron microscopy. The fractured surface of neat PLA shows mainly brittle fracture, indicated by smooth surfaces. In addition, some very thin and long polymer fibrils span over the surface (indicated with arrows). These might origin from a plastic fracture mechanism, allowing the material to yield and form long PLA fibrils. When the fibrils finally break they seem to buckle and fall onto the fractured surface. The same kind of PLA polymer fibrils was also observed on the fractured surface images of the composites and they should not be confused with the cellulose fibrils synthesized with the aim to reinforce the polymer matrix. Clearly, all cellulose fibrils (c-NFC, c-NFC-hex and c-NFC-hex$_{sm}$) showed excessive formation of low aspect ratio agglomerates. There is no evidence of a fibrillar network in either of the composites, even though the size of agglomerates clearly decreases in the order c-NFC (agglomerates with diameters in the range of approximately 300 μm and more were found) > c-NFC-hex (approximately 100 μm and lower) > c-NFC-hex$_{sm}$ (approximately 50 μm and lower). The images

of c-NFC-hex (Fig. 7c) and c-NFC-hex$_{sm}$ (Fig. 7d) also clearly show that the interaction/adhesion between the fibril agglomerates and the PLA is very poor.

In this study, a combination of several parameters might be the reason for the observed restricted reinforcement of PLA. First, the carboxymethylation of NFC decreased the crystallinity of the original nanofibers, and by that lowered the modulus of the fibrils. Second, the decreased strength of the composites with increased NFC contents indicated a poor interaction between the PLA and the cellulose nanofibers, modified or not. Third, a poor dispersion of the dried NFC powders inside the polymer matrix has been obtained during the extrusion. Apart from the poor fiber-matrix interface mentioned previously, this problem may also be linked with the preparation of the materials prior to the extrusion. Fourth, the use of surface charged cellulose nanofibers may have negatively impacted the thermal stability of the composite materials. In addition to the color change of PLA-c-NFC samples, MFI measurements and measurements of viscoelastic properties in shear of the polymer melts showed that the thermal stability of PLA was reduced when compounded with c-NFC. A possible explanation for these results may come from the reaction of carboxylate groups of c-NFC with the PLA at elevated temperatures (temperatures up to 200 °C were used in the extruder), therefore decreasing the thermal stability of the matrix. Moreover, it has been reported earlier that the presence of carboxylate groups leads to a decrease in the thermal stability of cellulose [18, 20, 21]. In addition, a degrading effect of DMAc/LiCl at elevated temperatures of 80–125 °C on cellulose was reported. The mechanism included the formation of keteniminium ions, inducing hydrolytic cleavage of the glycosidic bonds in cellulose [22]. This process was accompanied by a yellow coloration. Consequently in our study, a similar mechanism involving charged compounds might also be responsible for the limited stability of c-NFC.

Composites containing c-NFC-hex or c-NFC-hex$_{sm}$ were less susceptible to thermal degradation. This result might be related with a possible increased thermal stability of the esterified nanofibers as compared with c-NFC, and/or with the "blocking" of c-NFC carboxylate groups which therefore decreased the probability of PLA degradation. However, a reinforcing effect in terms of an increase in G' or viscosity was not found for any of the composites.

Conclusions

The aim of this study was to examine if dried nanofibrillated cellulose (NFC) in powder form, with different polarities, can be dispersed in PLA using an extrusion process, and to further evaluate its capacity to reinforce the PLA. To achieve our goal, different functionalized nanofibers were compounded with PLA using an extrusion process. Carboxymethylated NFC (c-NFC) was esterified with 1-hexanol in presence of a sulfuric acid catalyzer to yield c-NFC hexanoate (c-NFC-hex). In addition, a solvent mix (c-NFC-hex$_{sm}$) was prepared by mixing equal amounts of dissolved PLA and dispersed c-NFC-hex and precipitating the mixture in ice-cold isopropanol. Composites with different fibril contents were prepared by diluting the masterbatches of 10/90 (c-NFC/PLA, c-NFC-hex/PLA and c-NFC-hex$_{sm}$/PLA) with neat PLA to 2.5, 5 and 7.5 % w/w. The products were pelletized and injection molded to dog-bone shaped tensile test samples and flat discs for dynamic mechanical analysis and melt shear measurements. The fractured surfaces of the tensile test samples were analyzed by scanning electron microscopy.

The results showed that the types of fibrils examined in this work did not disperse, distribute or form a network within the PLA matrix but exhibited instead extensive agglomeration. Also, poor interaction with the matrix was observed in all composites, as demonstrated by DMA and SEM. The poor interaction and agglomerations affected the strength of the composites negatively. In addition, the thermal degradation of the PLA matrix, due to a possible reaction between the nanofibers carboxylate groups and the ester chains in high temperature, might also be a reason for the lowered mechanical properties of the composites. Furthermore, a decrease in crystallinity of the cellulose fibrils due to carboxymethylation could also have lowered the stiffness of the cellulose fibrils, and by that their reinforcing capability.

Even though this study on esterification of c-NFC with 1-hexanol for extrusion with PLA did not result in composite materials with increased mechanical properties, it should remain the subject of further research to find suitable and simple strategies for the development of composite materials with three-dimensional networks of nanofibrillated cellulose.

Acknowledgments The authors express their thanks to Aji Mathew and Maiju Hietala for their help during extrusion and injection molding, and Christian Walder (EMPA) for his support concerning the melt shear tests. The State Secretariat for Education and Research (SER) is gratefully acknowledged for the financial support of this work.

References

1. Auras R, Harte B, Selke S (2004) Macromol Biosci 4:835–864
2. Garlotta D (2001) J Polym Environ 9:63–84
3. Siro I, Plackett D (2010) Cellulose 17:459–494
4. Samir M, Alloin F, Dufresne A (2005) Biomacromolecules 6:612–626
5. Chazeau L et al (1999) J Appl Polym Sci 71:1797–1808
6. Favier V, Chanzy H, Cavaille JY (1995) Macromolecules 28: 6365–6367

7. Marchessault RH, Morehead FF, Walter NM (1959) Nature 184:632–633
8. Turbak AF, Snyder FW, Sandberg KR (1983) J Appl Polym Sci Symp 37:815–827
9. Oksman K et al (2006) Compos Sci Technol 66:2776–2784
10. Mathew AP et al (2006) In: Oksman K, Sain M (eds) Cellulose nanocomposites: processing, characterization, and properties. American Chemical Society, Washington, pp 114–131
11. Petersson L, Kvien I, Oksman K (2007) Compos Sci Technol 67: 2535–2544
12. Bondeson D, Oksman K (2007) Compos A Appl Sci Manuf 38: 2486–2492
13. Bondeson D, Oksman K (2007) Compos Interfaces 14:617–630
14. Iwatake A, Nogi M, Yano H (2008) Compos Sci Technol 68:2103–2106
15. Suryanegara L, Nakagaito AN, Yano H (2009) Compos Sci Technol 69:1187–1192
16. Tingaut P, Zimmermann T, Lopez-Suevos F (2010) Biomacromolecules 11:454–464
17. Jonoobi M et al (2010) Compos Sci Technol 70:1742–1747
18. Eyholzer C et al (2010) Cellulose 17:19–30
19. Lee K-Y, Blaker JJ, Bismarck A (2009) Compos Sci Technol 69: 2724–2733
20. Fukuzumi H et al (2009) Biomacromolecules 10:162–165
21. Leza ML et al (1989) Die Angewandte Makromolekulare Chemie 168:195–203
22. Rosenau T et al (2003) Polymer 44:6153–6158